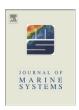


Contents lists available at SciVerse ScienceDirect

Journal of Marine Systems

journal homepage: www.elsevier.com/locate/jmarsys



An Individual Based Model of Arctic cod (*Boreogadus saida*) early life in Arctic polynyas: II. Length-dependent and growth-dependent mortality

Stéphane Thanassekos *, Dominique Robert, Louis Fortier

Québec-Océan, Département de Biologie, Université Laval, Québec, QC, Canada G1V 0A6

ARTICLE INFO

Article history: Received 9 December 2010 Received in revised form 30 July 2011 Accepted 2 August 2011 Available online 16 August 2011

Keywords: Individual-based model Larval fish Arctic cod Mortality Length-dependent Growth-dependent Sampling bias

ABSTRACT

A bioenergetics individual based model (IBM) of early growth is used to investigate the relative importance of length-dependent and growth-dependent mortality during the early life (0–45 d) of Arctic cod in the Northeast Water (NEW) in 1993 and the North Water (NOW) in 1998. In the model, individual growth is forced by the observed temperature and prey concentration histories as prescribed by the hatch date of a larva. The IBM reproduced well the observed length-at-age and revealed large ontogenetic and interregional fluctuations in instantaneous growth. Four mortality scenarios were compared for each population: (1) constant mortality (estimated from catch-at-age data); (2) length-dependent mortality; (3) growth-dependent mortality; and (4) combined length- and growth-dependent mortality. Scenarios 2, 3, and 4 were parameterized to achieve the final survival produced by the constant mortality rates estimated from observations (scenario 1). Scenario 2 accounted well for declining mortality with size but not for the large variations in growth-dependent mortality. Scenario 3 failed to capture the decreasing vulnerability of surviving larvae to predation. Only scenario 4 accounted for both the large fluctuations in growth-dependent mortality and the progressive shift in dominance from length-dependent to growth-dependent mortality as the survivors increased in size. Sub-sampling the model output to reproduce the limited temporal resolution of sampling at sea improved the fit between observed and modeled frequencies-at-age, and pointed to the undersampling of the smallest larvae as a major sampling bias.

© 2011 Elsevier B.V. All rights reserved.

1. Introduction

The high and variable mortality rate experienced by marine fish during the larval stage is considered the main determinant of a cohort's relative survival success (Govoni, 2005; Houde, 2009). The probability of surviving through this short period closely relates to individual growth performance (Anderson, 1988; Houde, 1987), Fast growing larvae would benefit from reduced vulnerability to predation and starvation mainly through a large size-at-age (e.g. bigger-isbetter hypothesis - Miller et al., 1988) and/or superior physiological condition at a given size (e.g. growth-selective predation hypothesis – Takasuka et al., 2003). Hence, at any time during drift in the plankton, population mortality would be a function of the size-at-age and growth rate of individuals (Hare and Cowen, 1997; Meekan et al., 2006). Fast growth and large size-at-age would be particularly important in cold seas where maximizing energy reserves (Heintz and Vollenweider, 2010; Hurst, 2007) and pre-winter size (Bouchard and Fortier, 2008; Fortier et al., 2006) is believed to increase the survival of juveniles over the first winter. Despite a growing body of field and laboratory evidence supporting the growth-mortality paradigm, quantifying variations in mortality rate throughout the larval stage remains a challenge (Jung et al., 2009; Jung and Houde, 2004; Tian et al., 2007).

Typically, the mortality suffered during early ontogeny is estimated by fitting an exponential decay model to catch-at-age data (e.g. Fortier and Quiñonez-Velazquez, 1998; Wang and Liu, 2006). Such catch curves assume that the mortality rate is constant through age. time, and among individuals (Ricker, 1975; Xiao, 2005), However, the rate of mortality is known to change during early development. generally decreasing after the transition from the yolk-sac stage to the post-yolk-sac stage, and again after metamorphosis into the juvenile form (e.g. Dahlberg, 1979). Since a large size is often correlated to fast growth, the relative contribution of size-dependent and growthdependent mortality to overall mortality during early life is difficult to assess from field data (Hare and Cowen, 1997; Meekan et al., 2006; Pepin, 1993). Individual-based models (IBM) of early growth and survival require the estimation throughout ontogeny of the changing probability that an individual will die (Cowan et al., 1996; Heath and Gallego, 1997; Letcher et al., 1996; Tian et al., 2007). Ideally, an IBM should reproduce the average estimated mortality of the population while simulating individuals characterized by a different probability of dying.

In the present study, we compare the effect of different parameterizations of mortality on the output of a bioenergetics IBM of the early growth of Arctic cod. The model was run with the mortality rate set in turn to (1) constant, (2) length-dependent, (3)

^{*} Corresponding author. E-mail address: stephane.thanassekos.1@ulaval.ca (S. Thanassekos).

growth-dependent, and (4) both length- and growth-dependent. The effect of the different mortality parameterizations on modeled growth (length-at-age and instantaneous growth) and mortality (instantaneous mortality rate, frequency-at-age and population survival over time) was assessed. The model output was sub-sampled to account for the absence in field collections from the Northeast Water and the North Water, of individuals of a given age hatched on a given date. The frequencies-at-age calculated from the sub-sampled and complete model outputs were compared to observations for each mortality parameterization.

2. Methods

2.1. Determination of variable mortality rates

The IBM simulated the early growth of two populations of 3 million virtual larvae each in the Northeast Water (NEW, Greenland Sea) in 1993 and the North Water (NOW, Baffin Bay) in 1998 respectively. The virtual larvae were hatched according to the hatch date frequency distribution observed in the two regions in those years. In the IBM, individual growth is forced by daily time series of observed spatially averaged temperature and prey concentrations. A mixed-feeding stage (yolk+prey) is followed by an exogenous feeding stage during which foraging ability increases with size (Thanassekos and Fortier, in press).

Sampling of fish larvae and zooplankton at sea and the resulting data sets used to force and validate the IBM were detailed previously (Thanassekos and Fortier, in press). In summary, 819 Arctic cod larvae were collected at 61 (positive) stations in the NEW and 1086 at 44 stations in the NOW. The age of all larvae collected in the NEW was determined either by otolith analysis (n = 444) or a length-age key (r^2 = 0.966) (Fortier et al., 2006). In the NOW, 459 larvae were aged by otolith analysis and 411 using an otolith diameter-age relationship (r^2 = 0.98, p < 0.0001, M. Ringuette, personal communication) for a total of 870 larvae aged.

In the model, instantaneous growth IG (mm d⁻¹) was defined as the daily increment in body length (L, mm):

$$IG_{(age)} = L_{(age)} - L_{(age-1)}$$
.

 $IG_{(0)}$ was randomly picked from a Normal distribution with parameters (mean and variance) set to reproduce the distribution of $IG_{(1)}$ as calculated by a preliminary model run.

Instantaneous mortality can be computed as a decreasing power or an exponential function of increasing length (see review in Jung and Houde, 2004). For each day of the simulation, the length-dependent instantaneous mortality rate IM_L (d⁻¹) of each individual was computed as:

$$IM_L = (1 - IM_{\min}) e^{-(L - L\min)/\alpha_L)} + IM_{\min}$$

where IM_{min} is the minimum mortality rate set at 0.01 d⁻¹, and α_L controls the slope of the decline in mortality with increasing length. L_{min} is the minimum length observed in the field (3.0 mm).

For each day of the simulation, the growth-dependent instantaneous mortality rate $IM_G(\mathrm{d}^{-1})$ of each individual was computed as:

$$IM_G = (1 - IM_{\min})e^{-IG(age)/\alpha_G} + IM_{\min}$$

where α_G controls the slope of the reduction in mortality with increasing growth. In the model, $IG \ge 0$ since starving individuals can lose weight but cannot shrink in length (Thanassekos and Fortier, in press).

The model was run with the mortality rate set in turns as constant (scenario 1), length-dependent (scenario 2), growth-dependent (scenario 3), and combined mortality (sum of length-dependent

and growth-dependent $IM_L + IM_G$, scenario 4). Based on catch-at-age data, the estimated average daily mortality rate was 14.5% d⁻¹ in the NOW (Thanassekos and Fortier, in press) and 13.9% d⁻¹ in the NEW (summer cohort, Fortier et al., 2006). These constant average mortality rates based on field observations were used in scenario 1 to estimate the final number of virtual larvae out of the initial 3 million that could be expected realistically to survive at the end of the simulation in each region. The simulation ended 10 days after the last date on which larvae were captured in each region (i.e. August 6 in the NEW and July 30 in the NOW). This final number of survivors was then reproduced (\pm 500 individuals) in scenarios 2, 3 and 4 by adjusting α_L and/or α_G . This approach ensured that the simulated final survival was realistic and enabled us to compare results among simulations in each region.

In scenario 4 (combined mortality), the relative importance of the length-dependent component and the growth-dependent component of the bi-dimensional mortality rate cannot be determined a priori, and α_L and α_G were reduced proportionally by maintaining the ratio α_L/α_G as close as possible to its value calculated from scenarios 2 and 3, to avoid double counting mortality. The death of an individual in the model was determined by comparing the daily individual instantaneous mortality rate IM (d $^{-1}$) to a random number n picked from a uniform distribution ($0 \le n \le 1$). If the value of the mortality rate exceeded the random number attributed to an individual i at a given time step t ($IM_{i,t} > n_{i,t}$), this individual was removed from the simulation.

2.2. Model validation based on observations at sea

The suboptimal sampling of natural systems is an important issue when validating model results with field observations (Gallego et al., 2007; Hannah, 2007). In the model, each survivor of the initial population of 3 million virtual larvae is tracked on a daily basis. By comparison, the age at capture is known for fewer than a thousand larvae collected at sea in each of the two regions studied. A consequence of low sample sizes and low sampling resolution at sea is that the daily cohorts that make up the larval population are not represented at all ages during the early life trajectory (Fortier et al., 2006; Fortier and Quiñonez-Velazquez, 1998). To assess the impact of this low resolution on the validation of the model, the model output was sub-sampled to reproduce this absence of daily cohorts at a given age (Thanassekos and Fortier, in press). For each simulation, the model generated two output matrices (Fig. 1). A complete matrix included all surviving virtual larvae from hatch to death. A second matrix retained only the virtual larvae that shared the age and the hatch date of a larva sampled at sea (Fig. 1). At the end of each simulation, the frequency-at-age (number of individuals of a given age divided by the overall number of modeled individuals) was calculated from both matrices and compared to the observations.

3. Results

3.1. Length-dependent and growth-dependent mortality in the different scenarios

In scenarios 2 (length-dependent mortality), 3 (growth-dependent mortality), and 4 (combined mortality), the slope factors (α) were adjusted to attain the same number of survivors at the end of simulations as in scenario 1 (constant mortality). In scenario 2, length-dependent mortality (IM_L) had a very similar slope (α_L) in the NEW and the NOW (Fig. 2a). IM_L declined exponentially with length from 1.00 d⁻¹ at 3.0 mm to a value of ca. 0.02 d⁻¹ at 14.5 mm (i.e. the mean length achieved at 45 d of age over the two regions). In scenario 3, growth-dependent mortality (IM_G) declined rapidly with increasing growth, reaching the asymptote of 0.01 d⁻¹ around a growth rate of 0.5 mm d⁻¹ in the NEW

Download English Version:

https://daneshyari.com/en/article/4548294

Download Persian Version:

https://daneshyari.com/article/4548294

<u>Daneshyari.com</u>